Materials Today Physics 31 (2023) 100969

Contents lists available at ScienceDirect

Materials Today Physics

journal homepage: www.journals.elsevier.com/materials-today-physics

Giant magnetoelectricity in soft materials using hard magnetic soft materials

Amir Hossein Rahmati [a,1], Rong Jia [b,1], Kai Tan [b], Liping Liu [c], Xuanhe Zhao [d,e], Qian Deng [f,**], Pradeep Sharma [a,g,*]

[a] Department of Mechanical Engineering, University of Houston, TX, 77204, USA
[b] School of Aerospace Engineering, Xi'an Jiaotong University, Xi'an, 710049, China
[c] Department of Mathematics and Mechanical and Aerospace Engineering, Rutgers University, NJ, 08854, USA
[d] Department of Mechanical Engineering, Massachusetts Institute of Technology, Cambridge, MA, 02139, USA
[e] Department of Civil and Environmental Engineering, Massachusetts Institute of Technology, Cambridge, MA, 02139, USA
[f] Department of Engineering Mechanics, School of Aerospace Engineering, Huazhong University of Science and Technology, Wuhan, 430074, China
[g] Department of Physics, University of Houston, Houston, TX, 77204, USA

A B S T R A C T

Imagine a material that will produce electricity via a contactless, wireless signal. Further, we hope that this material is capable of large deformation reminiscent of soft robots and is soft enough to conform to irregular or curved geometries. This would all be possible if soft magnetoelectric materials were available; paving the way for applications such as remote drug delivery, energy harvesting, soft robots, multiple state memories among others. Here, for the first time, using the concept of hard magnetic soft matter in combination with electrets, we design and create a soft magnetoelectric material that exhibits an extremely strong, self-biased magnetoelectric effect. Further, using programmable pattern of deposition of magnetic dipoles and charges, we report a giant magnetoelectric coefficient in an ultra-soft deformable material that retains its strength even under infinitesimal external fields and at low frequencies.

The magnetoelectric (ME) property is rare in single phase (natural) materials and restricted to certain hard exotic crystals that satisfy a stringent set of material symmetry constraints [1–3]. An alternative approach is to create artificial ME materials using composites of piezoelectric and magnetostrictive materials [4–8]. While such composites may exhibit significant magnetoelectricity [9–11], they are typically *hard* brittle materials and often painstakingly fabricated and frequently contain environmentally toxic materials such as lead. Even polymer based ME composites (in particular PVDF and its copolymers) which are regarded as lead-free, flexible and light weight class of ME composites, are not suitable candidate for applications in soft robotics, biology and medicine due to several reasons: First, truly *soft* ME composite do not exist! Even flexible PVDF based ME composites have elastic modulus on the order of several GPa and, therefore, are not really soft. Second, an *external* static bias-field is often necessary to achieve an appreciable ME coupling in composites and this renders the resulting devices quite bulky and hinges on the integration of electronics [12]. We emphasize that the magnetoelectric coefficient α of such materials (which embodies the strength of the interconversion between electrical and magnetic fields) is directly proportional to the externally applied magnetic field h^e, and thus becomes negligible for small fields unless a pre-existing static bias magnetic field is present. Finally, ME composites exhibit strong coupling only at high frequencies rendering them unsuited for wireless energy transfer for implantable medical devices where high frequency magnetic field may cause safety issues [13]. Examples of low frequency application of ME materials includes targeted drug delivery [14], brain stimulation [15], and tissue regeneration [16].

Recently, we have made some progress in creating soft ME materials based on silicone rubber by exploiting the so-called Maxwell stress effect and electrets [17,18]. Electrets are dielectric materials with embedded immobile electric charges and/or dipoles. We have shown that electret materials can exhibit a piezoelectric-like behavior if designed carefully [19–22]. While the fabricated materials were indeed mechanically soft, the magnetoelectric coefficient was modest especially under weak magnetic fields (and thus shares the same disadvantage as ME composites in that the magnetoelectric coefficient depends linearly on the

* Corresponding author. Department of Mechanical Engineering, University of Houston, TX, 77204, USA.
** Corresponding author. Department of Engineering Mechanics, School of Aerospace Engineering, Huazhong University of Science and Technology, Wuhan, 430074, China
E-mail addresses: tonydqian@hust.edu.cn (Q. Deng), psharma@uh.edu (P. Sharma).
[1] Contributed Equally.

https://doi.org/10.1016/j.mtphys.2023.100969
Received 4 October 2022; Received in revised form 13 December 2022; Accepted 7 January 2023
Available online 18 January 2023

external applied field ($\alpha \propto h^e$)).

In this work, however, we make a significant breakthrough. We use the concept of hard magnetic soft matter [23–25] and electrets (–referred in the following as hard magnetic soft electrets–HMSE). The inclusion of hard magnetic particle in soft rubbers has been exploited to induce large and fast actuation in soft materials [23], self-lubricating soft continuum robots [25] and soft magnetoelastic generator [26]. We have recently presented the theory of hard magnetic soft materials to create the ME effect [27] but there is no report of creation of soft magnetoelectric material using hard magnetic particles. HMSEs are soft materials in which magnetically hard micro particles and electric charges and dipoles are embedded in a way to exhibit non-uniform magnetic field strain (See Fig. 1). The electrets provide the basis for an apparent piezoelectric-like behavior. The reason for designing the material such that an imposed magnetic field generates a non-uniform deformation is that, non-uniformity of the deformation is essential for the exhibition of the apparent piezoelectric effect [19–21]. The reason for using hard magnetic particles instead of soft-magnetic particles is that hard magnetic materials have high coercivity which helps sustain the high residual magnetic flux density over a wide range of applied magnetic fields below the coercive field strength. Also, as our theoretical work shows (see *Methods* and *Supplementary Information (SI) Section*), in this concept, the mechanical strain ϵ is linearly proportional to magnetic field $\epsilon \propto B^r h^e$ and the magnetoelectric coefficient of these materials becomes independent of the externally applied magnetic field ($\alpha \propto q_0 B^r$). Here, B^r is the residual magnetic flux density due to hard-magnetic particles and q_0 is the electret charge density. Therefore, HMSEs can enable extremely large ME coupling coefficient even under extremely small magnetic fields and there is no need for a static bias field. The third reason for preference of the hard magnetic materials over soft magnetic materials is that the hard magnetic materials can be easily programmed to exhibit any kind of deformation pattern and therefore may be used to design programmed hard magnetic soft electrets. It is important to note that the magnetoelectric effect in HMSE materials relies on apparent piezoelectric property of the electret phase of the material. This enables conversion of magnetic field into electricity which is fundamentally different from magnetic induction that has been used in other works in the literature [26,28] in order to harvest electric energy from mechanical motion.

We show that guided by a rigorous theoretical and computational framework, HMSEs with giant ME voltage coupling coefficient $\alpha_{\mathrm{ME}}^{\mathrm{eff}} \geq 1$ can be designed and fabricated in a rather facile manner. Indeed, the fabrication scheme for the HMSEs is accomplished at low temperatures and amenable for small scale and miniaturized applications. We remark that any soft dielectric material can be used to as the basis for the HMSEs e.g. rubber. As we demonstrate, the ME effect can be designed (even optimized) by modifying the arrangement of electric charges/dipoles or altering the alignment of magnetic particles inside the material. Specifically, for a system made of an electret polytetrafluoroethylene (PTFE) thin film layered with micro-hard-magnetic particle embedded silicone rubber, we demonstrate a room temperature ME voltage coupling coefficient of 332.7 $\mathrm{mVcm^{-1}\ Oe^{-1}}$ at low frequency (1Hz) and zero bias field. Finally, upon programmed patterned magnetic dipoles (guided by theory), under flexure deformation mode, we are able to report a giant ME voltage coupling coefficient of 15.36 $\mathrm{Vcm^{-1}\ Oe^{-1}}$ at resonance frequency of 6 Hz in an elastically uniform material with elastic modulus of 55 KPa.[2] To the best of our knowledge, this is the only soft material fabricated so far which exhibits a "giant" ME effect. In fact, the ME coupling coefficient of our fabricated material is even comparable to the highest values reported in the literature for polymer based ME composite but with the caveat that our material is extremely soft (capable of large deformation), operable at low frequencies and no bias field is required (see and Fig. S1 in the *SI* for a comparison to other material systems.)

1. Emergent magnetoelectricity in tension-compression deformation mode

The materials preparation is described in *Methods*. In the simplest design, HMSE is composed of two disc shape layers. One layer consists of a neodymium-iron-boron microparticles (NdFeB) in the soft rubber (Ecofelx-0010) which we refer to as magnetic elastomer and the second one is polytetrafluoroethylene (PTFE) thin film sandwiched between two mechanically compliant electrodes (see inset of Fig. 2a and Fig. S2). A layer of surface charge was deposited onto one surface of the PTFE thin film by the corona charging technique to create the electret. PTFE is known to be better for electret charge stability [29]. In addition, since PTFE is not ferromagnetic, it hardly deforms under a magnetic field, while a nonzero deformation is developed in magnetic elastomer layer in response to an applied magnetic field. This non-uniform deformation is vital to the appearance of a electromechanical response in the material (see Eq. S8 in the SI). In order to compare the behavior of HMSEs with previously developed Soft Magnetic Soft Electrets (SMSEs) [17], we also fabricated and examined a SMSE sample by attaching a soft magneto-active rubber to a charged PTFE layer. The soft magnetoactive rubber which is referred to as iron embedded elastomer is a mixture of iron microparticles and soft rubber (see *Methods* for details on fabrication of SMSE samples and see Fig. S3 for the depiction of SMSE, HMSE and programmed HMSE).

The two layers of PTFE, magnetic elastomer layers behave differently in response to the applied magnetic field. The magnetic permeability of the PTFE layer is close to 1 and thus will not deform in response to the magnetic field. However, the magnetic elastomer layer will tend to expand (resp. contract) along the thickness direction if the applied field is in the same (resp. opposite) direction of the residual magnetic field. This behavior is due to the existence of hard magnetic particle inside the magnetic elastomer layer which leads to the existence of a large residual non-zero magnetic flux density inside this layer. The interplay between external and internal magnetic flux density thus leads to the deformation of the material. This behavior is consistent with our theoretical results (see Eqs. S6 and S7 in the *SI*). Therefore, magnetic elastomer layer will deform in response to magnetic field and PTFE layer remains almost undeformed. The non-uniform deformation in the electret material leads to an apparent piezoelectric effect in these materials [19,20,30]. Our theoretical results show that a strain mediated magnetoelectric effect is possible when two layers deform differently (see Eq. S8). This non-uniform deformation alters the electric field inside the material which, under short circuit boundary condition, leads to the transfer of electric charges from one electrode to the another. This magnetic field induced transfer of charges can be interpreted as the ME effect. It is important to note that this ME mechanism is sharply different from ME mechanism in conventional ME composites. The ME mechanism in composites relies on the transfer of strain from one phase to another, while the ME effect in HMSEs relies on non-uniform deformation. This is because existence of non-uniform deformation is essential for generation of piezoelectric effect in electret materials [19–21]. We have experimentally measured electric output charges generated as result of an alternating magnetic field with frequency of 1 Hz applied to both HMSE and SMSE samples. The output charge versus time is plotted in Fig. S4. Measured output charges are used to calculate the ME voltage coupling coefficient of material using the relation $\alpha_{\mathrm{ME}}^{\mathrm{eff}} = \frac{\partial(\Delta Q)}{C^{\mathrm{eff}} H \partial h^e}$, where ΔQ, H and C^{eff}, respectively, are the total output charges, total thickness and the effective capacitance of the material. The values of $C^{\mathrm{eff}} = 44.4$ pF and $C^{\mathrm{eff}} = 34.5$ pF have been experimentally measured for both HMSE and SMSE samples. Further details on experimental measurement of ME voltage coupling coefficient can be found in the SI. Fig. 2a shows the

[2] Technically, we do have a very thin teflon layer to stabilize the charge so there is a disruption in elastic non-uniformity but this is a rather localized and isolated disturbance.

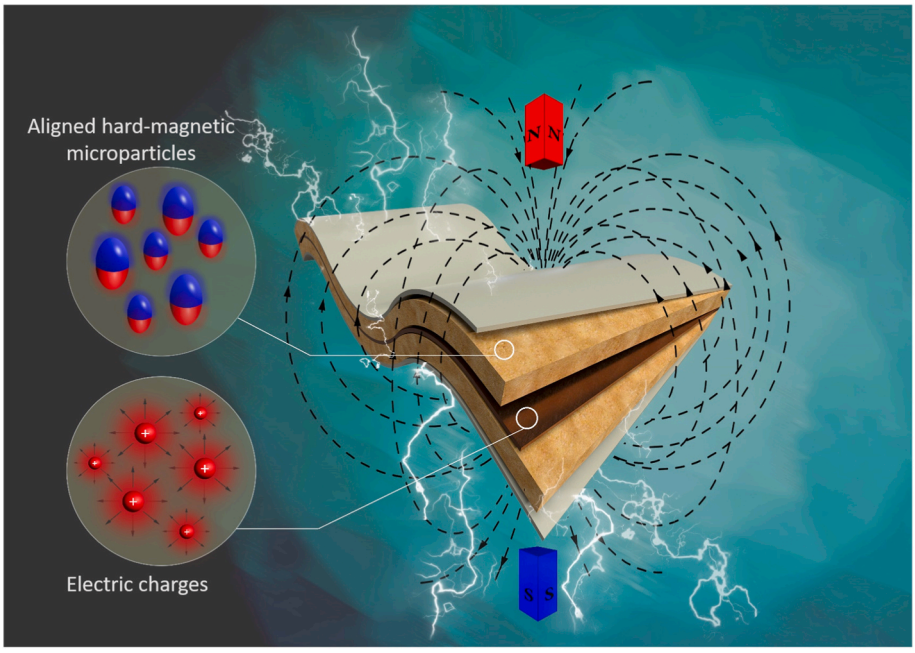

Fig. 1. A schematic illustration of Hard Magnetic Soft Electret (HMSE) materials. (a) HMSE materials fabricated in this work are composed of two layers of dielectric material(s) with a layer of embedded charges at the interface (electric charge shown with yellow circles with plus sign on the sphere). In addition to charges, magnetically-hard micro particle are embedded in top layer of the material. The material is sandwiched between two mechanically compliant electrodes. Magnetic dipoles may be patterned or programmed to mediate a desired strain-mediated magnetoelectric effect. (b) Applying magnetic field to this material leads to change in the electric polarization of the material. (For interpretation of the references to colour in this figure legend, the reader is referred to the Web version of this article.)

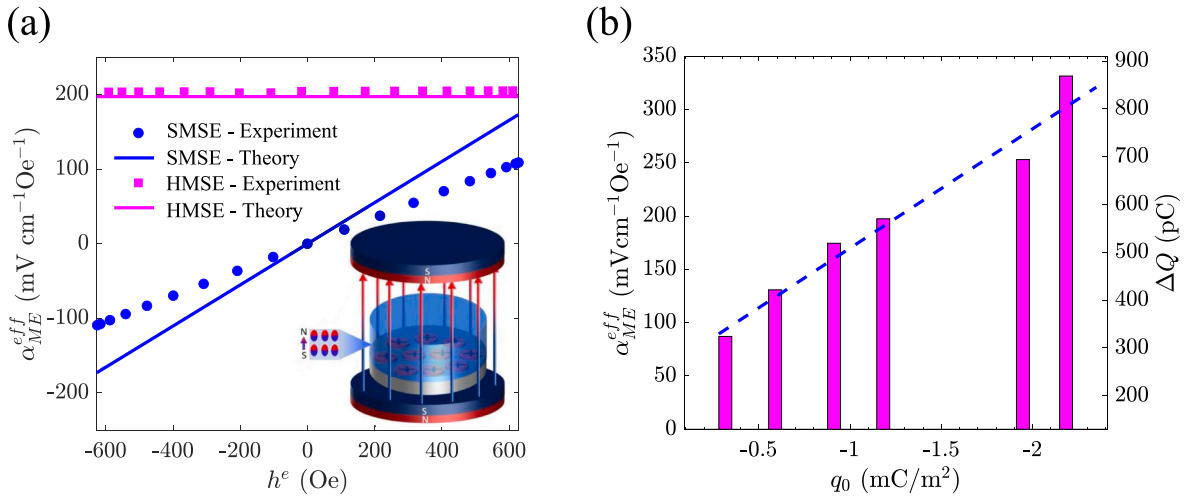

Fig. 2. (a) The ME voltage coupling coefficient of HMSE and SMSE measured at different magnetic fields. Inset of the figure shows the structure of HMSE which is made of two layers. NDFeB micro particle embedded soft rubber is on top and PTFE layer is on bottom and there is a layer of electric charges between two layers. (b) The ME voltage coupling coefficient of different HMSEs with different interfacial charge densities measured at $h^e = 627$ Oe.

voltage coupling coefficient of two samples for different magnetic fields. This figure also illustrates that the voltage coupling coefficient of the SMSE is linearly proportional to the magnetic field and, more importantly, it vanishes at zero magnetic field (as predicted by us). Therefore, SMSEs are similar to conventional ME composites, and show an exceedingly weak response for modest magnetic fields. This necessarily implies that a static bias magnetic field has to be used to increase the sensitivity of SMSEs. On the contrary, $\alpha_{\mathrm{ME}}^{\mathrm{eff}}$ of HMSE is constant with respect to external magnetic field, and is experimentally measured to be around 204 mV cm^{-1}Oe^{-1}, which is significant for practical applications [31]. As evident from the figure, our theoretical prediction of ME voltage coupling coefficient is consistent with experimental results (details of the theoretical approach is in the *Methods* section and *SI*). The mechanistic underpinnings for the distinct behavior of HMSEs compared to SMSEs and ME composites is further highlighted in Fig. S5 where we illustrate strain versus applied magnetic field for magnetic elastomer, iron embedded elastomer and magnetostrictive samples. We note a linear relationship between strain and external magnetic field for magnetic elastomer which is consistent with our theoretical predictions (see *SI*). However, magnetic field induced strain in ME composites and SMSE vary quadratically with the external magnetic field. As a result, output charge in SMSEs and ME composites depends quadratically on the external field. This behavior is also obvious from Fig. S3 where frequency of output charge in HMSE is the same as the frequency of external field while in SMSEs, the frequency of output charge is twice as large as the applied field. The linear relationship between external magnetic field and output charges for HMSE is shown in Fig. S6. As a result, the ME voltage coupling coefficient, which is the derivative of output charge with respect to magnetic field, is independent of external field in HMSEs.

According to our theoretical predictions (see *SI*), $\alpha_{\mathrm{ME}}^{\mathrm{eff}}$ can be improved by either increasing surface charge density or increasing residual magnetic flux density in the materials. Experimental results for these two strategies, respectively, are shown in Fig. 2b and Fig. S7. As we

can observe from Fig. 2b, α_{ME}^{eff} monotonically increases as the interface charge density of two layers increases. The linear dependence of α_{ME}^{eff} on the interface charge density is in agreement with theoretical prediction (Eq S8). The maximum surface charge density we are able to achieve experimentally is ≈ 2 mC/m^2 and the maximum ME voltage coupling coefficient we have achieved with this design of HMSE is 332.7 mV cm^{-1}Oe^{-1}. This value was measured at a very small frequency of 1 Hz. This result proves that ultra-soft HMSE materials can exhibit very strong ME effect in weak magnetic fields and under very small frequencies without the need for a DC bias magnetic field (see Fig. S8 for more info on mechanical properties of programmed HMSE). To the best of our knowledge, this is the first known soft material with such a compelling magnetoelectric effect without a DC bias magnetic field. In and Fig. S1 (*SI*), we may note that the ME effect of our fabricated material at such small frequency is comparable to the highest self biased ME voltage coupling coefficient achieved with polymer based ME composites.

2. Flexure deformation mode and "giant" magnetoelectricity

In the design of HMSE presented in the preceding section, the ME effect is mediated by tension and compression deformation of the material. Since non-uniform deformation is necessary to generate a piezoelectric like effect in electret materials, having a hard layer in the structure of HMSE (which hardly deforms with respect to the magnetoactive layer) is essential to achieve ME effect in the previous design for compression/tension. This stiffens the overall material somewhat (although the material is still *relatively* soft compared to other contenders like composites). However, the manifestation of electromechanical coupling in electret materials is not just restricted to compression/tension [21,32]. In a flexure mode, electrets can exhibit a large electromechanical effect regardless of whether they are elastically uniform (or not). The flexure deformation mode is also important because resonance frequency in bending deformation is much smaller than compression. Finally, we can theoretically show that in HMSEs designed in the tension and compression mode, we have $\alpha_{ME}^{eff} \propto B^r q_0$ and for HMSEs designed for the flexure mode, we have $\alpha_{ME}^{eff} \propto ARB^r q_0$ (see *SI*), where *AR* is the structural aspect ratio (typically greater than 10). Therefore, bending induced ME effect is at least one order of magnitude larger than tension/compression induced effect.

While it is difficult to achieve magnetic field induced bending deformation in SMSE materials, hard magnetic materials can be programmed to undergo any form of deformation in response to applied magnetic field. This provides an extensive design space for designing HMSEs with desirable deformation and enhanced ME property. To demonstrate this, we create a programmed HMSE (–abbreviated as programmed HMSE) which is designed to exhibit bending deformation in response to an applied magnetic field.

Fig. 3a represents the steps for creating programmed HMSE (with further details in *Methods*). The shape programmability in programmed HMSEs is achieved by deforming the material in the magnetization step (3a step II). Initially, the material is not magnetized which means the magnetic dipoles inside hard magnetic microparticles are randomly oriented (Fig. 3a step (I)). At this stage, we bend and fix the double-layer magnetoelastomer and apply a magnetic filed as high as 1.2 T to the material which leads to magnetization of hard magnetic materials along the direction of the external magnetic field which means magnetic dipoles inside magnetic particles reorient along the direction of the external field (Fig. 3a step (II)). Due to the high coercivity and high residual magnetic flux density of NdFeB micro particles, these materials stay magnetized and the magnetization profile remains stable even after the magnetic field has been turned off. Once the magnetization magnetic field is removed and the deformation is reversed, the magnetic micro

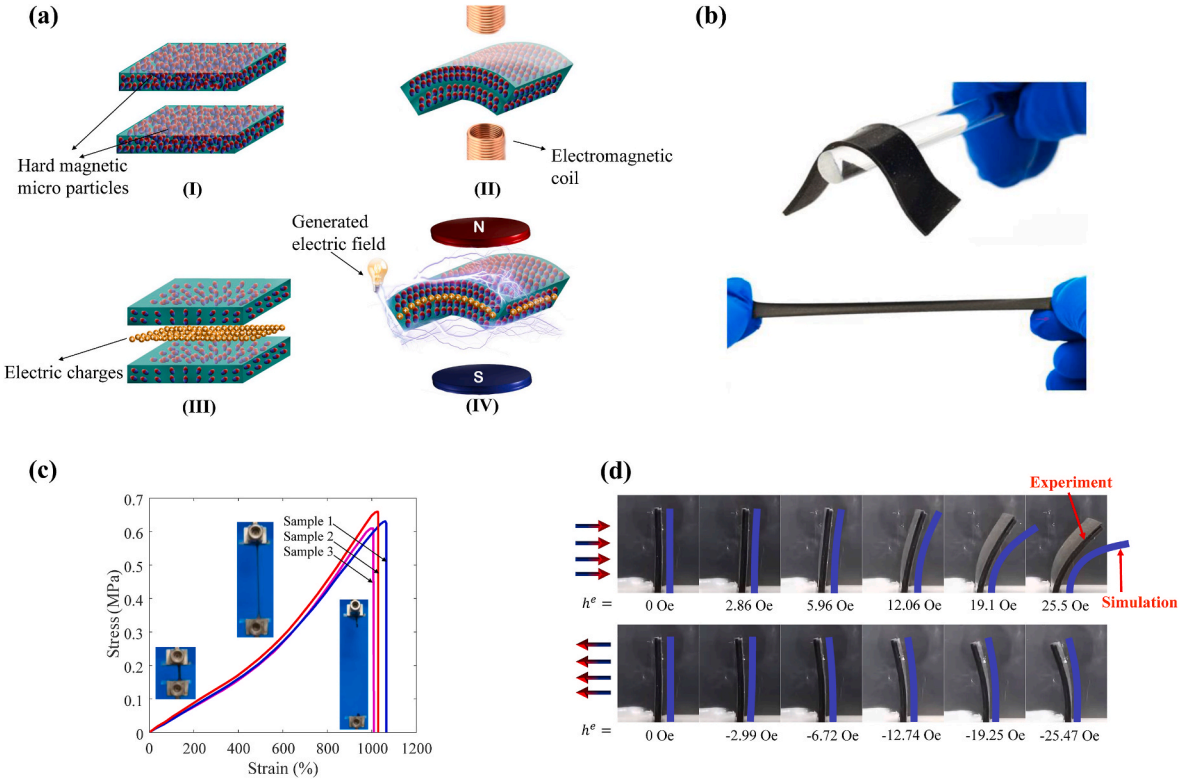

Fig. 3. (a) Steps for creating programmable hard magnetic soft electrets: (I) Initially magnetic dipoles inside the material are randomly oriented and residual magnetic flux density of the material is zero. (II) The material is deformed and a large magnetic field is applied to magnetize the material. (III) The material is undeformed and a layer of charges is deposited between two layers. (IV) A uniform magnetic field leads to ME effect. (b) The fabricated programmed HMSE specimen is highly deformable. (c) Stress-strain graph of three samples of magnetic elastomer. (d) Comparison of experimental and numerical simulation results for deformation under different static magnetic fields. A good agreement is observed between experimental results and simulations.

particles which are anchored to matrix material rotate as the material element rotates (Fig. 3a step (III)). As shown in Fig. 3a step (III), a layer of electric charges are inserted in the middle of the material using a very thin charged PTFE material and then all layers of the material are stuck together. We remark that since the thickness of PTFE is negligible compare to thickness of the overall material, overall the material is essentially elastically uniform. For further information on reorientation process of hard magnetic particles inside the material, we refer the reader to references [24,33,34]. The highest residual flux density achieved is $B^r = 0.0767$ T. The profile of the residual flux density has been theoretically calculated in Eq. (4). It should be mentioned that the residual magnetic flux density is expected to increase with increasing concentration of hard magnetic particles but this could potentially impact the charge stability and it increase the stiffness of the material. Moreover, we also expect shape and orientation of magnetic particles to impact the magnetoelastic behavior of hard magnetic soft electrets. Although there is no study on the homogenization of hard magnetic soft electrets, Danas [35] presented a homogenization theory for effective properties of magnetoelastic composites. Also, Liu and Sharma [20] presented homogenization theory for soft electret materials. These works can be used to further optimize the ME response of hard magnetic soft electrets but such discussions are beyond the scope of this work. The fabricated programmed HMSE material has dimensions $22 \times 12 \times 1.85$ mm, $C^{eff} = 6.40$ pF and $q_0 = 0.0488$ mC/m^2 unless otherwise stated. The softness of the fabricated material may be readily (and visually) appreciated from Fig. 3b. In addition, Fig. 3c shows the stress-strain response of the magnetic elastomer indicating that the material can be stretched more than 10 times its size (– its elastic modulus is roughly 55 KPa). Also, the mechanical testing results of the programmed HMSE material is shown in Fig. S9 where it is seen that insertion of PTFE layer (which has been added for charge stability reason) does not hugely impact deformability of the material and still the material has the maximum elongation of more than 600%.

We show the deformation behavior of programmed HMSE under a uniform static magnetic field in Fig. 3d. As a uniform vertical field is applied to material, the magnetic particles tend to align themselves along the applied external field. The alignment of the particle occurs by deformation of the material as these hard-magnetic particles are anchored to the material points. Therefore, the whole material bends in response to applied magnetic field. The curvature of the material increases as the magnetic field increases (Fig. 3d). As the structure bends, material points above the neutral axis are under compression and the remainder are under tension. This non-uniform deformation in the electret material leads to an apparent piezoelectric effect. Therefore, a magnetic field generates an electric signal resulting to magnetoelectric effect. The deformation is asymmetric with respect to the magnetic field since the residual field is not symmetric with respect to neutral axis of the beam. In addition to experimental results, we have also used numerical computation of our nonlinear fully coupled electro-magneto-mechanical theory to study the behavior of programmed HMSEs (see *Methods* and *SI* for details on the computational approach). As evident from Fig. 3d, our numerical results are in good agreement with experimental results.

We measure frequency response of the programmed HMSE by applying an alternating external magnetic field to the programmed HMSE. Fig. 4a shows the ME voltage coupling coefficient and the output charge of the programmed HMSE in response to an external magnetic fields with amplitude of 12 Oe and the frequency of 1–10Hz. As fully anticipated by our theory, no ME effect is in evidence if the sample is not charged. The resonance frequency of programmed HMSE is near 6 Hz where the output charge reaches its peak value. At the peak point, we obtain a giant ME voltage coupling of $\alpha_{\mathrm{ME}}^{\mathrm{eff}} \approx 11.2$ V cm^{-1}Oe^{-1}. We emphasize that we obtain this extraordinarily large ME effect at low frequency and without any external static bias field. In addition, the leakage current of the programmed HMSE has been measured and results are given in Fig. S9a. Also, Fig. S9b shows HMSE have very small leakage current compare to other multiferoic materials and devices. The effect of the magnitude of the applied alternating magnetic field on the ME coupling of the material is shown in Fig. 4b which illustrates that the output charge increases linearly with increase of amplitude of external field and ME voltage coupling coefficient of the material remains almost unchanged. This implies that our fabricated programmed HMSEs can exhibit giant ME coupling at extremely weak magnetic fields.

Similar to HMSEs, the $\alpha_{\mathrm{ME}}^{\mathrm{eff}}$ of programmed HMSEs can be further increased by increasing charge density. Fig. 5a reveals there is a linear relationship between interface surface charge density and the voltage coupling coefficient of the material. As charge density increases, ΔQ and $\alpha_{\mathrm{ME}}^{\mathrm{eff}}$ increase. We have been able to achieve a value of $\alpha_{\mathrm{ME}}^{\mathrm{eff}} = 15.36$ Vcm^{-1}Oe^{-1} when the static charge density is equal to 0.078 mC/m^2. To the best of our knowledge, this is the first soft material created with giant ME voltage coupling. This is one of the largest self biased ME voltage coupling coefficients even when compared with polymer based ME composites (see and Fig. S1).

The programmed HMSEs are not mechanistically different from HMSEs in this sense that their ME effect is strain mediated. The trends seen in the output charge behavior of programmed HMSE follows exact the trends as seen for deflection (see Figs. S10 and 4a). Any two external stimuli which result in the same deformation will lead to same electric

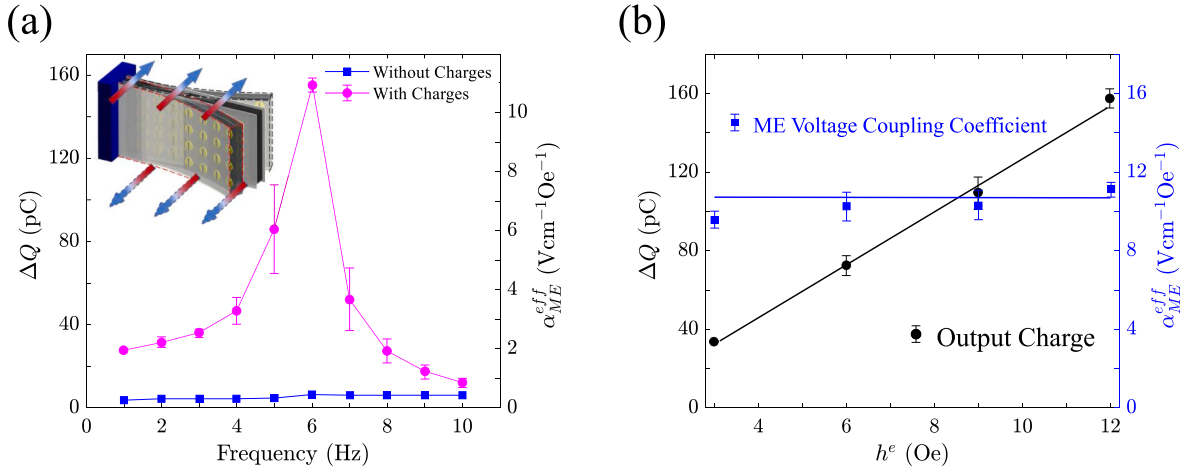

Fig. 4. (a) ME voltage coupling coefficient and output charge for charged programmed HMSE and non-charged sample under different frequencies. The results have been obtained by applying alternating magnetic field of amplitude $h^e = 12$ Oe. (b) The ME voltage coupling coefficient and output charge of programmed HMSE under magnetic fields with different amplitudes but the same frequency of 6 Hz.

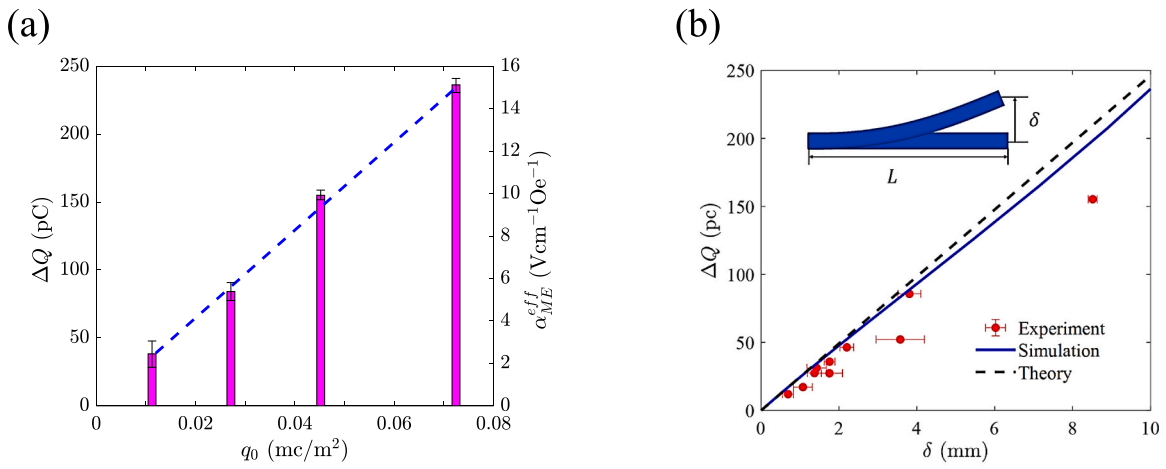

Fig. 5. (a) Effect of interfacial surface charge density on the ME voltage coupling coefficient and output charge of programmed HMSE under alternating magnetic field with the frequency of 6 Hz and amplitude of 12 Oe. (b) The deflection (curvature) versus output charge.

signal. To better show this insight, the deflection versus output charges obtained from experimental observation is shown in Fig. 5b. The experimental results have been obtained by applying magnetic fields with different frequencies but the same amplitude. In addition, we also plot the deflection versus output charge obtained from our numerical simulations conducted for the static condition in which different deflections obtained by applying magnetic field with different magnitudes. We remark that we have previously shown that, for an electret under pure symmetric bending, the output charges can be determined as $\Delta Q = A\frac{1}{4}q_0 H\kappa$, where A, H and κ are, respectively, surface area of the electrode, thickness of the material and curvature of the material. We can use this relation for cantilever beam to obtain a rough analytical relation between curvature and output charge. Curvature of a cantilever under pure bending can be roughly approximated as $\kappa = \frac{2\delta}{L^2}$, where δ is the tip deflection and L is the length. Therefore, the output charge may be roughly approximated as $\Delta Q = Aq_0 H\frac{\delta}{2L^2}$. This relation has been used in Fig. 5b to make a closed-form analytical prediction. Interestingly, despite the obvious approximations, we obtain a very good agreement between experimental, analytical and numerical results in Fig. 5b. From this, we arrive at two conclusions: First, the ME effect in programmed HMSEs is strain mediated. Second, the relation $\Delta Q = A\frac{1}{4}q_0 H\kappa$ can be used to obtain a reasonably good approximation for charge curvature relationship and electret materials can be used as a soft curvature sensor (for instance, in the context of biomedical applications).

3. Discussion

The magnetic field can induce large deformation in hard-magnetic soft-materials. Taking recourse to a simplified one dimensional model, such a strain generated in a hard-magnetic elastomer in response to the applied magnetic field scales as

$$\epsilon \approx \frac{B^r h^e}{3G}, \tag{1}$$

where B^r is the residual magnetic flux density of the material and G denotes the shear modulus of the material (See *SI* for further details). While the strain depends quadratically on the external magnetic field ($\epsilon \propto (h^e)^2$) in both magnetostrictive materials and soft magnetic elastomers, the magnetic field induced strain in hard-magnetic soft elastomers varies *linearly* with the external magnetic field h^e according to Eq. (1). The linear magnetic field strain relation signifies that HMSEs, unlike SMSEs and magnetoelectric composites, are able to sense the direction of the magnetic field. Moreover, for a bi-layer HMSE similar to the one shown in the inset of Fig. 2a where one layer is magnetoactive and the other layer hardly deforms in response to external magnetic field, we can determine the effective magnetoelectric voltage coupling coefficient as

$$\alpha_{\mathrm{ME}}^{\mathrm{eff}} = -\frac{1}{\epsilon^{\mathrm{eff}}}\frac{q_0 H_t H_b \varepsilon_b \varepsilon_t}{(H_t\varepsilon_b + H_b\varepsilon_t)^2} \times \frac{B_t^r}{3G_t}, \tag{2}$$

where subscript "t" and "b" refer to the materials used for top and bottom layers, respectively. Also, H and ε, respectively, denote thickness and electric permittivity of the material and q_0 is the surface charge density used at the interface of the two materials. Eq. (2) shows that the effective magnetoelectric voltage coupling coefficient of the HMSE is independent of the external magnetic field. This is consistent with the results presented in Fig. 2a. Therefore, the HMSE are suitable for sensing and energy harvesting applications under weak magnetic fields as their magnetoelectric coupling coefficient does not vanish as the magnetic field approaches to zero. Moreover, the relation (2) shows that any two arbitrary dielectric materials can be used to fabricate a HMSE as long as the following three conditions are met: (1) One of the materials must mechanically be soft in which hard magnetic micro/nanoparticles are embedded. (2) The second material must be elastically stiffer that it hardly deforms in response to the external magnetic field. (3) A layer of electric charges must be present (electret). The aforementioned considerations present a novel paradigm to engineer magnetoelectric effect in soft materials using *any* two arbitrary soft dielectric materials through a straightforward and low cost fabrication scheme.

Furthermore, we have also shown that we may even relax the constraint for elastic mismatch by using the programmable property of the hard magnetic soft materials and designing the material in a manner that a uniform magnetic field induces a nonuniform deformation (e.g. flexure). We have used this programmable feature and presented a programmed HMSE which bends in response to uniform magnetic field. As a small magnetic field can lead to a large bending deformation, the programmed HMSE fabricated by us exhibited a giant magnetoelectric effect.

In summary, we have presented HMSE materials as a new member of the family of the magnetoelectric materials. We have reported HMSE materials as the first known soft and stretchable materials which exhibit a giant self-biased magnetoelectric effect. Although there is ample opportunity for optimization and improvement of the magnetoelectric effect in these materials, we have shown that the magnitude of the magnetoelectric voltage coupling coefficient of the programmed HMSEs is comparable to highest values reported for magnetoelectric voltage coupling coefficients of polymer based magnetoelectric composites under low frequencies (see Table S1 and Fig. S1). While the choice for the piezoelectric phase in nearly all polymer based magnetoelectric composites is restricted to PVDF (and its co-polymers), any soft

dielectric material can be used to fabricate HMSE and programmed HMSE in a low cost and low temperature fabrication scheme. Future research direction could involve exploiting interplay with temperature c. f. [36,37], instabilities and energy harvesting c. f. [38], and exploiting liquid inclusions and capillary effects [39,40].

4. Methods

4.1. Fabrication of disk shape HMSEs and SMSEs

The magnetic elastomer is prepared by mixing NdFeB microparticles with silicone elastomer (Ecofle×00–10) at prescribed weight fraction (NdFeB particles: Ecoflex00-10 = 1:1). The mixture is poured into a mold to obtain desired geometry and the cured at 80 °C for 10 min. The final disk shape magnetic elastomer has the diameter of 40 mm and thickness of 1 mm (Fig. S2). A nonzero residual flux density is achieved in the material by applying a magnetization field with magnitude of 1 T. The magnitude of residual flux density of magnetic elastomer layer is $B^r = 0.058$T and its direction is align with the thickness direction of the material. The magnetic elastomer layer is attached to a disk shape PTFE layer with the thickness of 30 μm and the same thickness as magnetic elastomer layer. Before bonding two layers together, a layer of electric charges is deposited onto one surface of the PTFE thin film by the corona charging technique (Fig. S11). During the corona charging, a voltage difference of 5.7 kv is applied between the conductive needle and the grid (see (Fig. S11) which leads to ionization of air and movement of charges toward PTFE layer. The surface charge density of PTFE layer q_0 is measured by measuring the electric potential on the surface of the PTFE layer V_s using an electrostatic voltmeter (TRek MODEL P0865). The V_s and q_0 are related through

$$q_0 = \frac{\varepsilon^{\text{eff}} V_s}{H}, \tag{3}$$

where ε^{eff} is the effective electric permittivity of the material. Unless otherwise stated, the surface charge density achieved for all samples was $q_0 = -1.95$ mC/m^2. More details on mechanism of corona charging is found in the SI.

4.2. Fabrication of programmed HMSE

The steps for fabrication of programmed HMSE is illustrated in Fig. 3. In the first step, we mix the NdFeB particles with silica gel (Ecoflex 0020) in equal proportion to obtain the turbid solution. Thin magnetoactive elastomers is prepared by centrifugal suspension coating. Then, by cutting, and stick the two layers of magnetic elastomers together, we obtain double layer magnetoactive elastomers with size of the 22× 12 × 1.85 mm. At this stage, the magnetic particles inside the material are randomly oriented and overall residual magnetic field of the material is zero. In order to program the material in a way that it bends in response to external magnetic field, we bend the material and place it in a magnetic field with magnetic flux density of 1.2 T. The radius of curvature is 11.14 mm. After removal of the magnetic field, the bending deformation is reversed. Using the model presented by Rivlin [41] for the flexure of rectangular incompressible block, the profile for residual magnetic flux density in the material is determined as [21].

$$\widetilde{\mathbf{B}}^r = \mathbf{F}_{\text{b}}^{-1}\left[-B^r \cos\left(\frac{(2Y-L)\alpha}{L}\right)\mathbf{e}_r + B^r \sin\left(\frac{(2Y-L)\alpha}{L}\right)\mathbf{e}_\theta \right], \tag{4}$$

where $\mathbf{F}_{\text{b}}$ is the deformation gradient for the bending deformation of the rectangular block. Also, L represents length of the block (beam) and $0 \leq Y \leq L$. In addition, B^r is the magnitude of the residual magnetic flux density α is the bending angle applied in the magnetization step. Unless otherwise stated, $B^r = 0.0767$ and $\alpha = 52^\circ$. Next, we debond two layers of the material from each other and a charged PTFE layer between two layers of magnetoactive elastomer and bond three layers together. Insertion of PTFE layer is just for stability of electric charges and we have divided PTFE layer into smaller pieces so that it does not constrain softness and stretchability of the material. The charge density of the interface is $q_0 = -0.048$ mC/m^2 unless otherwise stated. Finally, we coat the sample surface with liquid metal as electrode.

4.3. Measurement of material properties

Electroforce 3230 - TA testing machine is used to perform uniaxial testing and determine Young's modulus of the material. The effective capacitance of the material C^{eff} is determined using an impedance analyzer (Keysight E4990A, America). The relation $C^{\text{eff}} = \varepsilon^{\text{eff}} A/H$ is used to determine the effective dielectric properties ε^{eff} of the material, where H is the thickness of the material and A is the surface area. Also, the reidual magnetic flux density B^r is related to magnetization M^r with the relation $B^r = \mu_0 M^r$. The magnetic hysteresis loop ($h^e - M^r$) was plotted by Vibrating Sample Magnetometer MPMS-squid VSM-094. Fig. S12 shows the magnetic hysteresis loops for both hard magnetic and soft magnetic particles.

4.4. Measurement of the magnetic field induced deformation and the output charges

A customized solenoid is used to generate the alternating magnetic field. Unless otherwise stated, magnetic field with amplitude of 627 Oe and frequency of 1 Hz is used for disk shaped HMSEs and magnetic field with amplitude of 12 Oe and frequency of 6 Hz is used to study programmed HMSEs. The magnetic field induced deformation is measured using a Laser Scanning Vibrometer (Polytec OFV-5000, Germany). The output charge of the material is measured using a charge amplifier (Bruel & Kjaer 2692, Denmark). The measurement equipment and diagram are shown in Figs. S13 and S14, respectively.

4.5. Theoretical modeling of the HMSEs

We use energy formulation to derive governing equations for magneto-electro-elastic behavior of a HMSEs. The distinction between reference configuration Ω_R and current configuration Ω is essential for capturing electro-mechanical coupling in the electret materials theoretically. Therefore, conventional linear elasticity models are unable to capture ME effect in the HMSEs and we have to use a nonlinear coupled formulation. Based on the principle of minimum free energy, the equilibrium state of the system is the state that minimizes free energy of the system. Using the deformation χ and the polarization $\mathbf{p}$ as two independent thermodynamic variables, We express free energy of the system as

$$\mathcal{F}[\chi, \mathbf{p}] = \int_{\Omega_R} W^{\text{elast}} + \int_{\Omega} \frac{|\mathbf{p}|^2}{2(\varepsilon - \varepsilon_0)} + \int_{\Omega} \frac{\varepsilon_0}{2}|\mathbf{e}|^2 - \int_{\Omega_R} \mathbf{F}\widetilde{\mathbf{B}}^r \cdot \mathbf{h}^{\text{e}}, \tag{5}$$

where ε, ε_0 and $\mathbf{h}^{\text{e}}$ are, respectively, electric permittivity of the material, electric permittivity of the vacuum and external magnetic field. Also, W^{elast} denotes elastic energy density of the material and $\mathbf{F}$ is the deformation gradient tensor. Our theory is based on the premise that the equilibrium state of the system must satisfy the Maxwell equation. The Maxwell equation for a material with charge density ρ_e in the current configuration is expressed as

$$\text{div}(\varepsilon_0 \mathbf{e} + \mathbf{p}) = \rho_e \qquad \text{in} \quad \Omega. \tag{6}$$

We use standard calculus of variation to derive Euler-Lagrange equations and boundary conditions for the equilibrium state of the system. More details on the theoretical modeling of the HMSEs can be found in the *SI Section*.

4.6. Computational modeling of programmed HMSEs

Based on the nonlinear coupled formulation discussed earlier, we develop a finite element model in order to study ME effect in programmed HMSEs. We use open source finite element software FEniCS [42] to implement finite element formulation. We derive weak form of the governing equations of the system and encode weak formulation in Python using mathematical operators available in FEniCS. The FEniCS meshing component mshr which allows capability of defining subdomains is used to create mesh for this problem. We assume the material is incompressible and use neo-Hookean constitutive equation for elastic behavior of the material. The numerical values for material properties is consistent with the values obtained using our experimental measurement. More details on the finite element implementation, meshing and validation of the numerical solution are available in the *SI Section*.

Declaration of competing interest

The authors declare that they have no known competing financial interests or personal relationships that could have appeared to influence the work reported in this paper.

Data availability

Data will be made available on request.

Acknowledgments

Authors PS and AR acknowledge support from the University of Houston and the Hugh Roy and Lillie Cranz Cullen Distinguished University Chair. Author Q.D. acknowledges support from the National Natural Science Foundation of China (12172142).

Appendix A. Supplementary data

Supplementary data to this article can be found online at https://doi.org/10.1016/j.mtphys.2023.100969.

References

[1] H. Schmid, Multi-ferroic magnetoelectrics, Ferroelectrics 162 (1) (1994) 317–338.
[2] N.A. Hill, Why are there so few magnetic ferroelectrics? J. Phys. Chem. B 104 (29) (2000) 6694–6709.
[3] K. Bhoi, H. Mohanty, M.F. Abdullah, D.K. Pradhan, S.N. Babu, A. Singh, P. Vishwakarma, A. Kumar, R. Thomas, D.K. Pradhan, et al., Unravelling the nature of magneto-electric coupling in room temperature multiferroic particulate (pbfe 0.5 nb 0.5 o 3)–(co 0.6 zn 0.4 fe 1.7 mn 0.3 o 4) composites, Sci. Rep. 11 (1) (2021) 1–17.
[4] C.W. Nan, M. Li, J.H. Huang, Calculations of giant magnetoelectric effects in ferroic composites of rare-earth–iron alloys and ferroelectric polymers, Phys. Rev. B 63 (14) (2001): 144415.
[5] C.W. Nan, M. Li, X. Feng, S. Yu, Possible giant magnetoelectric effect of ferromagnetic rare-earth–iron-alloys-filled ferroelectric polymers, Appl. Phys. Lett. 78 (17) (2001) 2527–2529.
[6] J. Ryu, S. Priya, A.V. Carazo, K. Uchino, H.-E. Kim, Effect of the magnetostrictive layer on magnetoelectric properties in lead zirconate titanate/terfenol-d laminate composites, J. Am. Ceram. Soc. 84 (12) (2001) 2905–2908.
[7] J. Ryu, A.V. Carazo, K. Uchino, H.-E. Kim, Magnetoelectric properties in piezoelectric and magnetostrictive laminate composites, Jpn. J. Appl. Phys. 40 (8R) (2001) 4948.
[8] S. Dong, J.-F. Li, D. Viehland, Ultrahigh magnetic field sensitivity in laminates of terfenol-d and pb (mg 1/3 nb 2/3) o 3–pbtio 3 crystals, Appl. Phys. Lett. 83 (11) (2003) 2265–2267.
[9] G. Srinivasan, E. Rasmussen, R. Hayes, Magnetoelectric effects in ferrite-lead zirconate titanate layered composites: the influence of zinc substitution in ferrites, Phys. Rev. B 67 (1) (2003): 014418.
[10] S. Dong, J. Zhai, N. Wang, F. Bai, J. Li, D. Viehland, T.A. Lograsso, Fe–ga/pb (mg 1/3 nb 2/3) o 3–pb ti o 3 magnetoelectric laminate composites, Appl. Phys. Lett. 87 (22) (2005): 222504.
[11] J. Zhai, S. Dong, Z. Xing, J. Li, D. Viehland, Giant magnetoelectric effect in metglas/polyvinylidene-fluoride laminates, Appl. Phys. Lett. 89 (8) (2006): 083507.
[12] H. Palneedi, D. Maurya, L.D. Geng, H.-C. Song, G.-T. Hwang, M. Peddigari, V. Annapureddy, K. Song, Y.S. Oh, S.-C. Yang, et al., Enhanced self-biased magnetoelectric coupling in laser-annealed pb (zr, ti) o3 thick film deposited on ni foil, ACS Appl. Mater. Interfaces 10 (13) (2018) 11018–11025.
[13] S. Kopyl, R. Surmenev, M. Surmeneva, Y. Fetisov, A. Kholkin, Magnetoelectric effect: principles and applications in biology and medicine–a review, Materials Today Bio (2021): 100149.
[14] M. Nair, R. Guduru, P. Liang, J. Hong, V. Sagar, S. Khizroev, Externally controlled on-demand release of anti-hiv drug using magneto-electric nanoparticles as carriers, Nat. Commun. 4 (1) (2013) 1–8.
[15] T. Nguyen, J. Gao, P. Wang, A. Nagesetti, P. Andrews, S. Masood, Z. Vriesman, P. Liang, S. Khizroev, X. Jin, In vivo wireless brain stimulation via non-invasive and targeted delivery of magnetoelectric nanoparticles, Neurotherapeutics (2021) 1–16.
[16] S. Ribeiro, C. Ribeiro, E.O. Carvalho, C.R. Tubio, N. Castro, N. Pereira, V. Correia, A.C. Gomes, S. Lanceros-Méndez, Magnetically activated electroactive microenvironments for skeletal muscle tissue regeneration, ACS Appl. Bio Mater. 3 (7) (2020) 4239–4252.
[17] K. Tan, X. Wen, Q. Deng, S. Shen, L. Liu, P. Sharma, Soft rubber as a magnetoelectric material—generating electricity from the remote action of a magnetic field, Mater. Today 43 (2021) 8–16.
[18] Z. Alameh, Q. Deng, L. Liu, P. Sharma, Using electrets to design concurrent magnetoelectricity and piezoelectricity in soft materials, J. Mater. Res. 30 (1) (2015) 93–100.
[19] Q. Deng, L. Liu, P. Sharma, Electrets in soft materials: nonlinearity, size effects, and giant electromechanical coupling, Phys. Rev. 90 (1) (2014): 012603.
[20] L. Liu, P. Sharma, Emergent electromechanical coupling of electrets and some exact relations—the effective properties of soft materials with embedded external charges and dipoles, J. Mech. Phys. Solid. 112 (2018) 1–24.
[21] A.H. Rahmati, S. Yang, S. Bauer, P. Sharma, Nonlinear bending deformation of soft electrets and prospects for engineering flexoelectricity and transverse (d 31) piezoelectricity, Soft Matter 15 (1) (2019) 127–148.
[22] A.H. Rahmati, L. Liu, P. Sharma, Homogenization of electrets with ellipsoidal microstructure and pathways for designing piezoelectricity in soft materials, Mech. Mater. 173 (2022): 104420.
[23] Y. Kim, H. Yuk, R. Zhao, S.A. Chester, X. Zhao, Printing ferromagnetic domains for untethered fast-transforming soft materials, Nature 558 (7709) (2018) 274–279.
[24] R. Zhao, Y. Kim, S.A. Chester, P. Sharma, X. Zhao, Mechanics of hard-magnetic soft materials, J. Mech. Phys. Solid. 124 (2019) 244–263.
[25] Y. Kim, G.A. Parada, S. Liu, X. Zhao, Ferromagnetic soft continuum robots, Science Robotics 4 (33) (2019).
[26] Y. Zhou, X. Zhao, J. Xu, Y. Fang, G. Chen, Y. Song, S. Li, J. Chen, Giant magnetoelastic effect in soft systems for bioelectronics, Nat. Mater. 20 (12) (2021) 1670–1676.
[27] A.H. Rahmati, R. Jia, K. Tan, X. Zhao, Q. Deng, L. Liu, P. Sharma, Theory of hard magnetic soft materials to create magnetoelectricity, J. Mech. Phys. Solid. (2022): 105136.
[28] X. Zhang, J. Ai, Z. Ma, Z. Du, D. Chen, R. Zou, B. Su, Magnetoelectric soft composites with a self-powered tactile sensing capacity, Nano Energy 69 (2020): 104391.
[29] S. Gong, J. Zhang, C. Wang, K. Ren, and Z. Wang, "A Monocharged Electret Nanogenerator-Based Self-Powered Device for Pressure and Tactile Sensor Applications," *Advanced Functional Materials*, p. 1807618, 01 2019..
[30] Z. Alameh, Q. Deng, L. Liu, and P. Sharma, "Using electrets to design concurrent magnetoelectricity and piezoelectricity in soft materials," J. Mater. Res., vol. 30, pp. 93–100, 01 2014..
[31] P. Martins, S. Lanceros-MenNdez, Polymer-based magnetoelectric materials, Adv. Funct. Mater. 23 (27) (2013) 3371–3385.
[32] X. Wen, D. Li, K. Tan, Q. Deng, S. Shen, Flexoelectret: an electret with a tunable flexoelectriclike response, Phys. Rev. Lett. 122 (14) (2019): 148001.
[33] X. Gong, K. Tan, Q. Deng, S. Shen, Athermal shape memory effect in magnetoactive elastomers, ACS Appl. Mater. Interfaces 12 (14) (2020) 16930–16936.
[34] D. Garcia-Gonzalez, M. Hossain, Microstructural modelling of hard-magnetic soft materials: dipole–dipole interactions versus zeeman effect, Extreme Mechanics Letters 48 (2021): 101382.
[35] K. Danas, Effective response of classical, auxetic and chiral magnetoelastic materials by use of a new variational principle, J. Mech. Phys. Solid. 105 (2017) 25–53.
[36] R. Mbarki, N. Baccam, K. Dayal, P. Sharma, Piezoelectricity above the curie temperature? combining flexoelectricity and functional grading to enable high-temperature electromechanical coupling, Appl. Phys. Lett. 104 (12) (2014): 122904.
[37] F. Darbaniyan, K. Dayal, L. Liu, P. Sharma, Designing soft pyroelectric and electrocaloric materials using electrets, Soft Matter 15 (2) (2019) 262–277.
[38] S. Yang, X. Zhao, P. Sharma, Avoiding the pull-in instability of a dielectric elastomer film and the potential for increased actuation and energy harvesting, Soft Matter 13 (26) (2017) 4552–4558.
[39] S. Krichen, L. Liu, P. Sharma, Liquid inclusions in soft materials: capillary effect, mechanical stiffening and enhanced electromechanical response, J. Mech. Phys. Solid. 127 (2019) 332–357.
[40] A. Mathur, P. Sharma, R. Cammarata, Negative surface energy—clearing up confusion, Nat. Mater. 4 (3) (2005) 186, 186.
[41] R. Rivlin, Large elastic deformations of isotropic materials. v. the problem of flexure, Proc. Roy. Soc. Lond. Math. Phys. Sci. 195 (1043) (1949) 463–473.
[42] A. Logg, K.-A. Mardal, G. Wells, Automated Solution of Differential Equations by the Finite Element Method: the FEniCS Book, vol. 84, Springer Science & Business Media, 2012.